Hubble bubble or Hubble trouble?

Antonio Enea Romano, UDEA/CERN

EPL 109 (2015) no.3, 39002
JCAP 1911 (2019) no.11, 016
Int.J.Mod.Phys. D27 (2018)

The "local" value of H_0 is obtained from low redshift supernovae (SN): 72.24

The "large scale" H_0value from CMB: 66.93

H_0 is constrained by CMB mainly through the distance to the last scattering

They are quite different..

Why?

Could it be the effect of a local inhomogeneity?

Evidence for a ~300 Megaparsec Scale Under-density in the Local Galaxy Distribution, Keenan et all, Astrophys.J. 775 (2013) 62

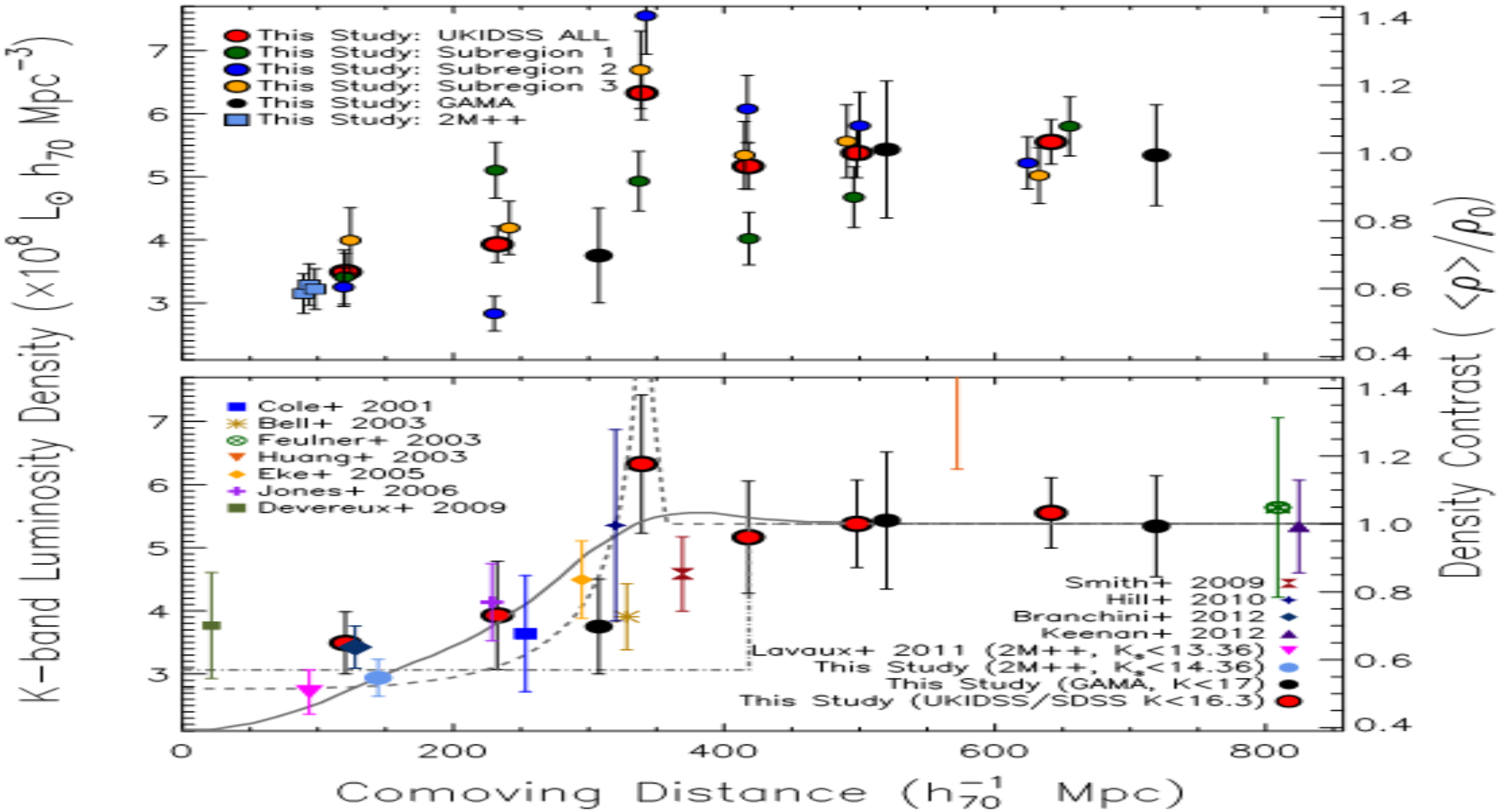

SN angular distribution

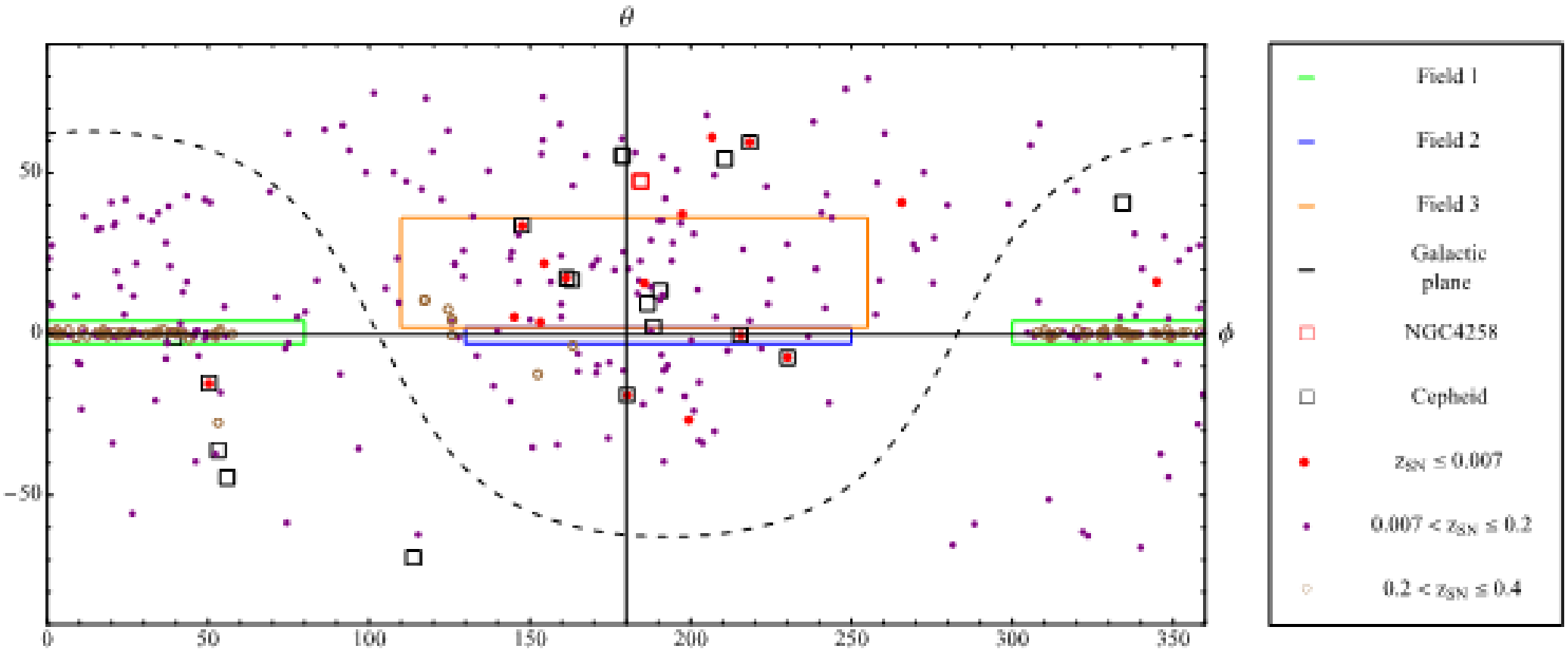

40% of Cepheids used for SN calibration are inside Field 3, direction along which Keenan found a significant radial inhomogeneity

Standard estimation of the effects of inhomogeneities on H_0,

E. L. Turner, R. Cen and J. P. Ostriker, *ApJ* **103** (May 1992)

$$a = a_b(1-\epsilon) = a_b + \delta a$$

$$d(\rho a^3) = d\rho\, a^3 + 3\rho\, a^2 da = 0,$$

$$\delta = \frac{\delta\rho}{\rho} = -3\frac{\delta a}{a} = 3\epsilon$$

$$H = \frac{\dot{a}}{a} = \frac{\dot{a}_b}{a_b} - \dot{\epsilon} = H_b - \frac{1}{3}\dot{\delta} = H_b + \Delta H\,.$$

$$\delta(t) = A(x)D(t)$$

$$H_b = \frac{\dot{a}_b}{a_b}$$

$$\Delta H = -\frac{1}{3}\dot{\delta}\,.$$

$$\frac{\Delta H}{H_b} = -\frac{1}{3} f\delta\,.$$

$$f = \frac{1}{H_b}\frac{\dot{D}}{D}\,.$$

Do we really measure the scale factor directly?

No… we measure the luminosity distance

$$\chi(z) = \frac{c}{H_0\sqrt{|\Omega_k|}} S_k\left(\sqrt{|\Omega_k|} H_0 \int_0^z \frac{dz'}{H(z')}\right) \qquad D_A(z) = \frac{\chi(z)}{(1+z)}, \qquad D_l(z) = (1+z)\chi(z)$$

So we should compute the effects of Inhomogeneities on D(z) not on a(t)!

Perturbative effects effects of inhomogeneities on D(z)

In the Newton gauge $$a^2\left[-(1+2\Psi)d\eta^2+(1-2\Phi)\gamma_{ij}dx^i dx^j\right]$$

linear perturbations calculations give, (Phys.Rev. D85 (2012) 029901)

$$\begin{aligned}\bar{d}_L(z_S,\mathbf{n}) = (1+z_S)(\eta_O-\eta_S)\Bigg\{&1-\frac{1}{(\eta_O-\eta_S)\mathcal{H}_S}\mathbf{v}_O\cdot\mathbf{n}-\left(1-\frac{1}{(\eta_O-\eta_S)\mathcal{H}_S}\right)\mathbf{v}_S\cdot\mathbf{n}\\ &-\left(1-\frac{1}{(\eta_O-\eta_S)\mathcal{H}_S}\right)\Psi_S-\frac{1}{(\eta_O-\eta_S)\mathcal{H}_S}\Psi_O\\ &+\frac{2}{(\eta_O-\eta_S)}\int_{\eta_S}^{\eta_O}d\eta\Psi+\frac{2}{(\eta_O-\eta_S)\mathcal{H}_S}\int_{\eta_S}^{\eta_O}d\eta\dot{\Psi}-2\int_{\eta_S}^{\eta_O}d\eta\frac{(\eta-\eta_S)}{(\eta_O-\eta_S)}\dot{\Psi}+\int_{\eta_S}^{\eta_O}d\eta\frac{(\eta-\eta_S)(\eta_O-\eta)}{(\eta_O-\eta_S)}\ddot{\Psi}\\ &-\int_{\eta_S}^{\eta_O}d\eta\frac{(\eta-\eta_S)(\eta_O-\eta)}{(\eta_O-\eta_S)}\nabla^2\Psi\Bigg\}.\end{aligned}$$

Dominating effects : covergence and Dopple

$$D_A(z) = \overline{D}_A(z)\,[1 - k(z)]$$

$$k(z) \approx k_\delta(z) + k_v(z)\,,$$

$$k_v = \left[1 - \frac{1}{a_e \chi_e H_e}\right] v_e \cdot n + \frac{1}{a_e \chi_e H_e} v_o \cdot n\,,$$

$$k_\delta = \frac{3}{2} H_0^2 \Omega_m \int_0^{\chi_e} \mathrm{d}\chi \frac{(\chi_e - \chi)}{a_e \chi_e} \chi \delta(\chi)\,,$$

$$v(\chi) = \frac{a f H}{4\pi} \int^{R_{Max}} \delta(\chi') \frac{\chi' - \chi}{|\chi' - \chi|^3} d^3\chi'\,.$$

The monopole of the effect on v depends on the volume average of the density contrast, as expected from Newtonian physics

$\delta = A(x)D(t)$, and $f = \frac{1}{H}\frac{\dot{D}}{D}$

$$v(\chi) = -\frac{1}{3} a f H \overline{\delta}(\chi)\chi\,,$$

$$\overline{\delta}(\chi) = \frac{3}{4\pi\chi^3} \int^{\chi} 4\pi\chi'^2 \delta(\chi')\, d\chi'$$

Low red-shift approximations : a local modification of Hubble law

$$aH\chi \approx z \qquad k_v(z) = -\frac{1}{3} f\bar{\delta}(z)\,. \qquad k_\delta = \frac{3}{4}\Omega_m \delta_c z^2$$

$$D_A(z) = D_L(z) = \overline{D_L}(z)\left[1 + \frac{1}{3} f\bar{\delta}(z)\right]$$

- The effect is negligible far from the homogeneity because of the volume average
- A local inhomogeneity affects the local estimation but not the large scale value of H_0

Effects of local estimation of the Hubble parameter

$$H_0^{loc} = \lim_{z \to 0} \frac{z}{D_L(z)}$$

$$\frac{\Delta H(z)}{\overline{H}_0} = -\frac{\Delta D_L(z)}{\overline{D}_L(z)} = -\frac{1}{3} f \overline{\delta}(z)$$

The effect can be quite different from the the formula used before based on the scale fact a(t)

$$\frac{\Delta H}{H_b} = -\frac{1}{3} f \delta$$

What kind void could resolve the apparent Hubble tension?

$$f = \Omega_m^{0.5512} \text{ and } D_A/\overline{D}_A \approx \Delta H/\overline{H}_0 \approx 9.4$$

$$\text{volume averaged density contrast } \delta \approx -0.57$$

- This value is in agreement with Keenan's analysis
- The void should extend beyond 2M++ depth, explaining why red-shift correction applied by Riess did not remove its effect
- This kind of inhomogeneity are found in LCDM simulations

Effects for non compensated void

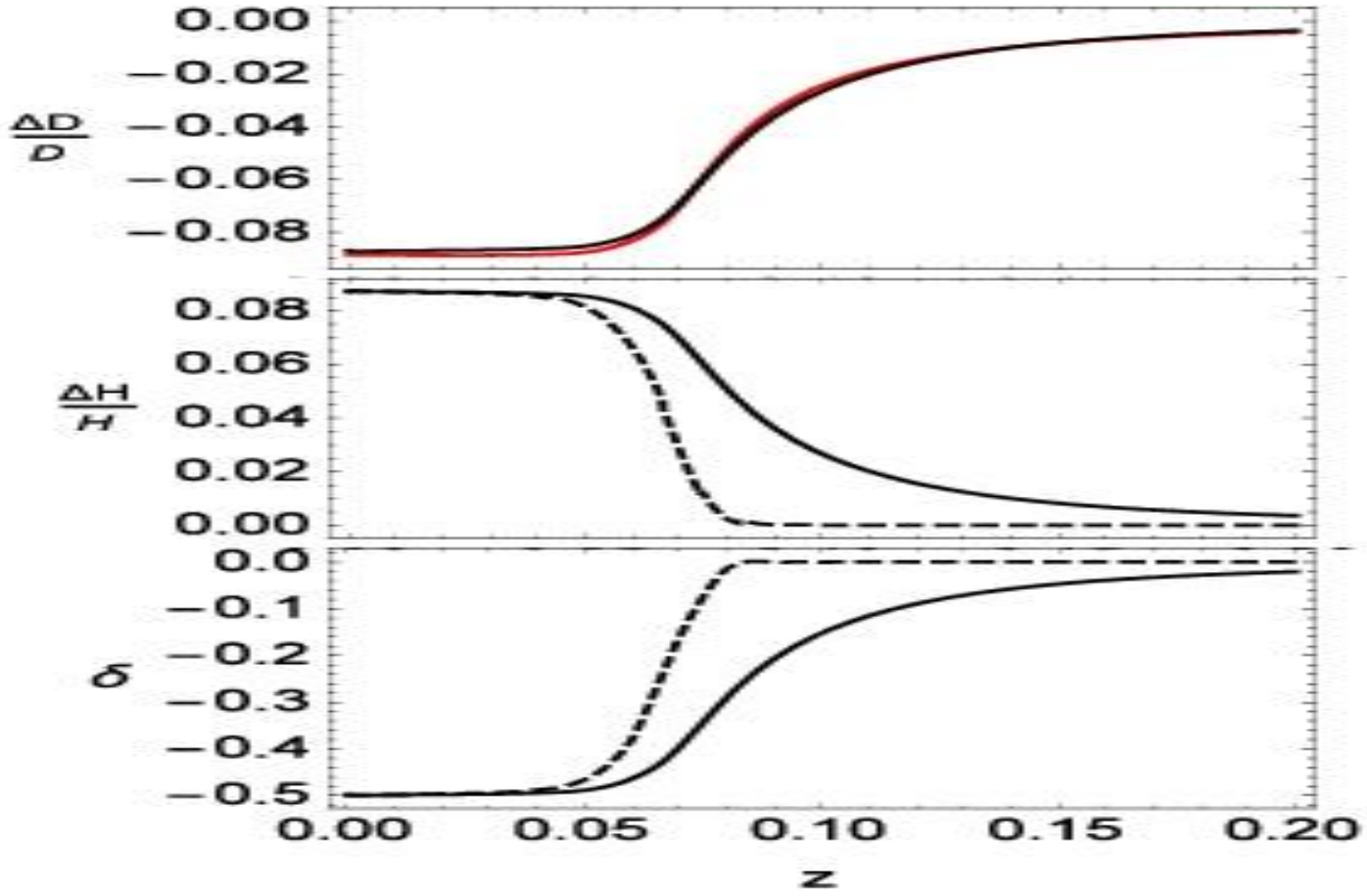

Effects for compensated void

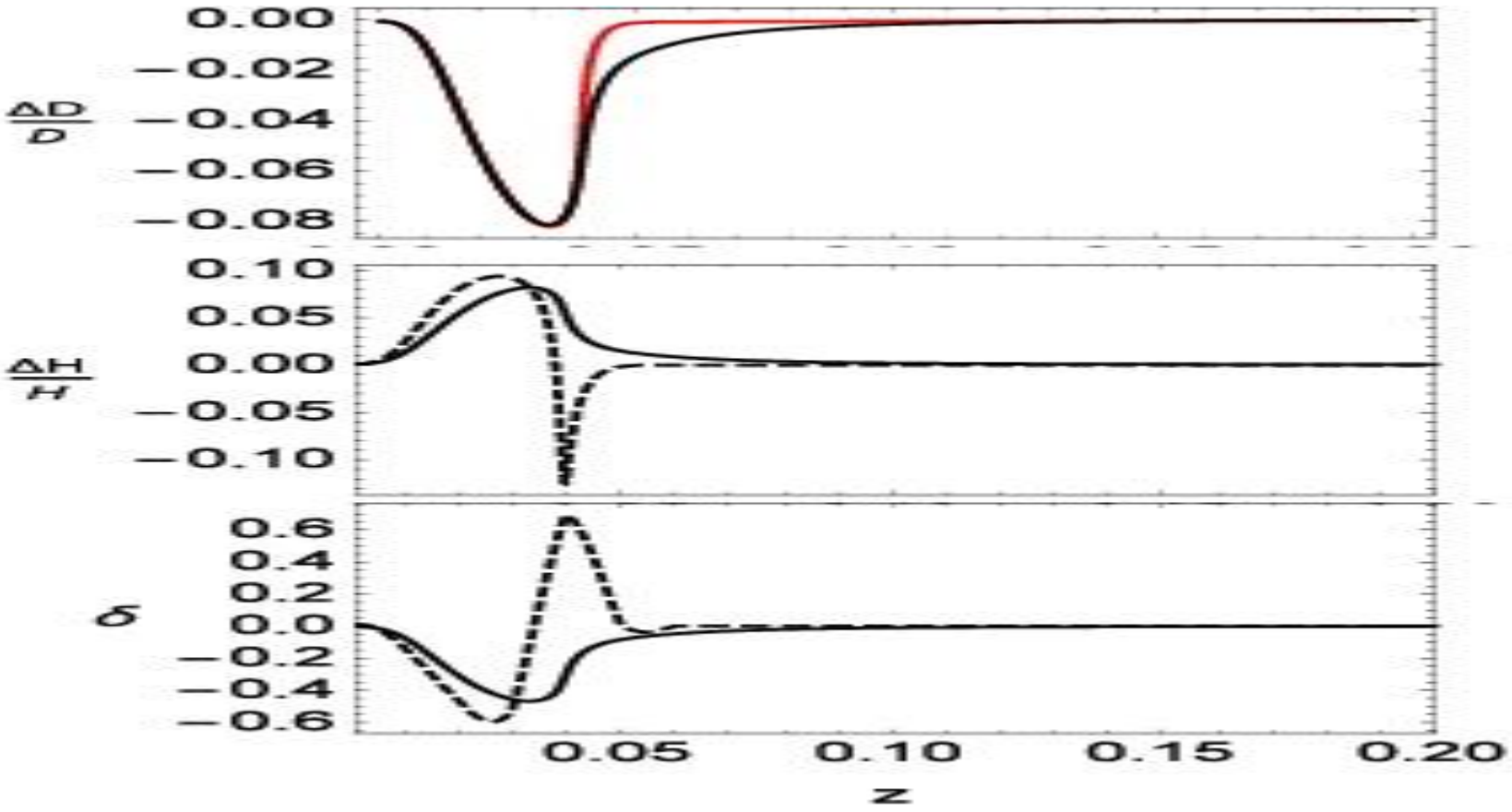

SN red-shift correction

$$D_A(z) \approx \overline{D}_A(z)\,[1-k_v] \approx \overline{D}_A(z)\left[1-\frac{v_e\cdot n}{z}\right]$$

$$D_A(z) \approx \overline{D}_A\,(z-\delta z)$$

$$v = v_{loc} + v_{LS}\,,$$

$$v_{loc} = \frac{afH}{4\pi}\int^{R_{max}} \delta_{loc}(\chi')\frac{\chi'-\chi}{|\chi'-\chi|^3}d^3\chi'\,.$$

$$v_{LS} = \frac{afH}{4\pi}\int^{R_{max}} \delta_{LS}(\chi')\frac{\chi'-\chi}{|\chi'-\chi|^3}d^3\chi'$$

$$\frac{\delta z}{z} = -\frac{1}{3}f\overline{\delta}(z)\,.$$

But 2M++ depth is only 0.06 …

Velocity profile inside a void

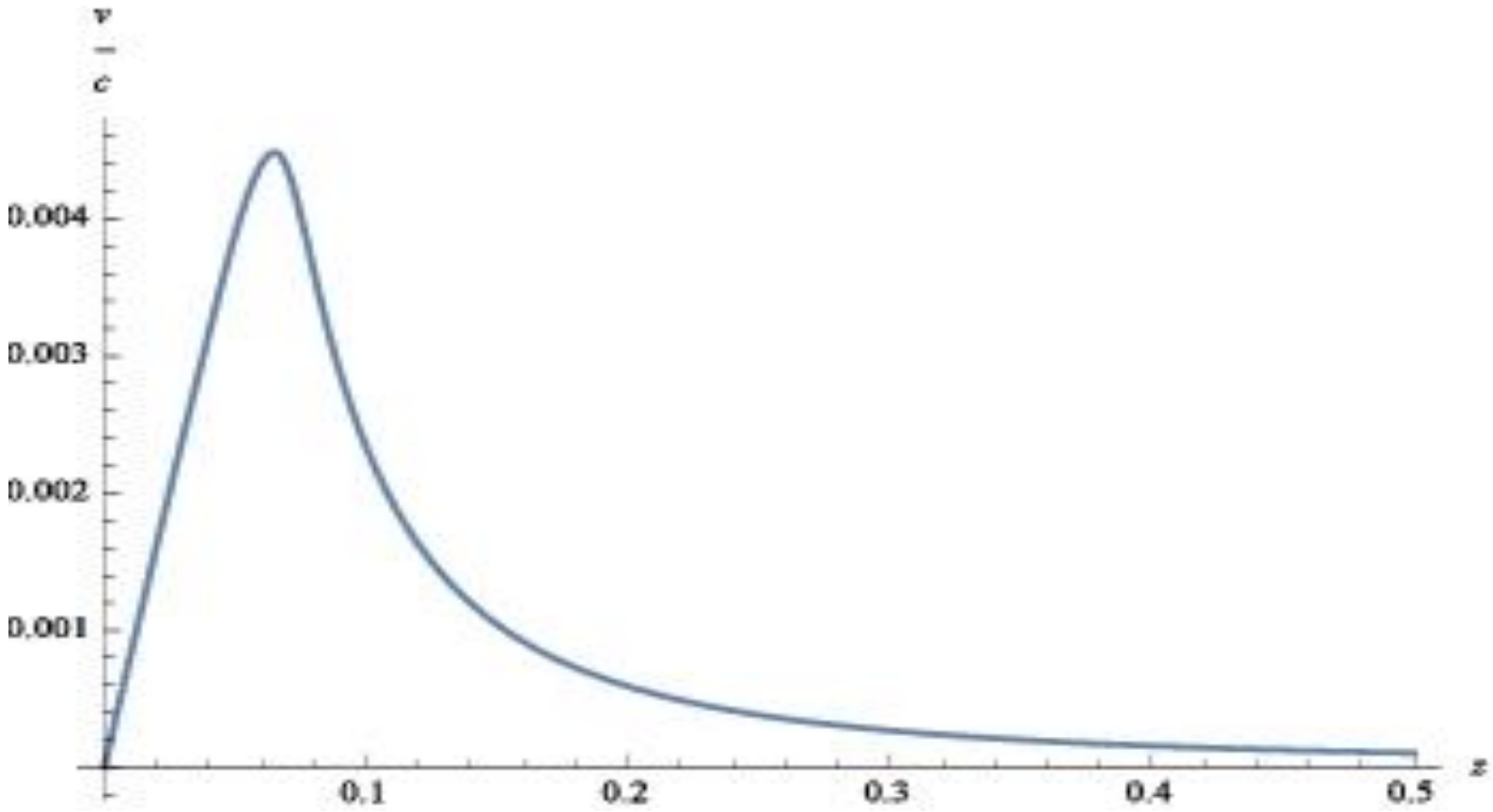

Reconstructing the high red-shift structure of the Universe with Supernovae

$$\bar{\delta} = \frac{3}{f}\left(1 - \frac{D_A}{\bar{D}_A}\right)\frac{1}{(aH\chi - 1)}$$

$$\delta(\chi) = \frac{1}{3}(\chi\bar{\delta}' + 3\bar{\delta}) \approx \frac{1}{3}\left[\chi\frac{d\bar{\delta}}{dz}\left(\frac{d\chi}{dz}\right)^{-1} + 3\bar{\delta}\right]$$

- This method opens a unique window at high red-shift large scale structure
- It can detect dark matter presence up to a red-shift 1.5 with Euclid

Anisotropy of local structure

- The Universe is not homogeneous on small scales, and assuming it is while it is not produces miss estimations of background cosmological parameters .. such as
- In the case of SN, there is an additional directional dependence due to the fact that their angular distribution is not uniform
- Keenan's results show that the radial density profile is not the same in all directions
- We have applied the inversion method to reconstruct independently the density profiles from SN data, confirming the anisotropy detected by Kenan using luminosity density

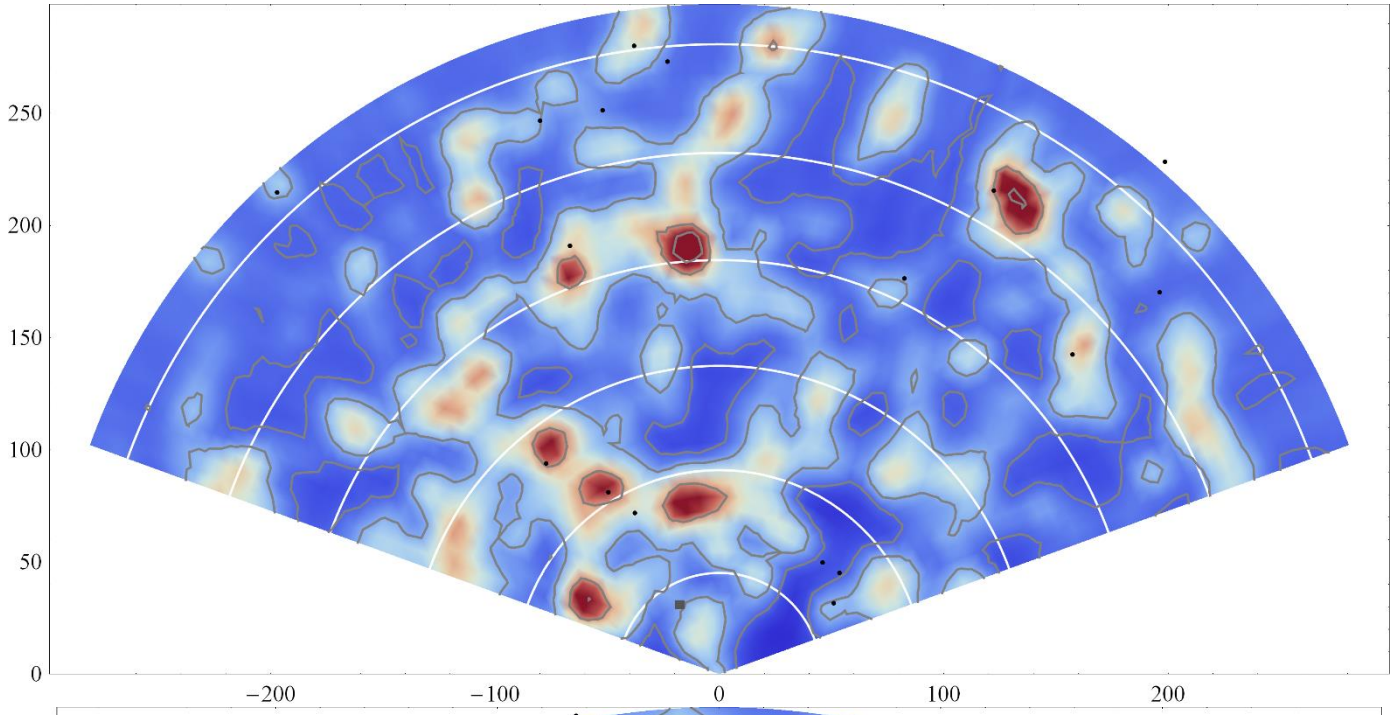

SN and Cepheids distribution in F1

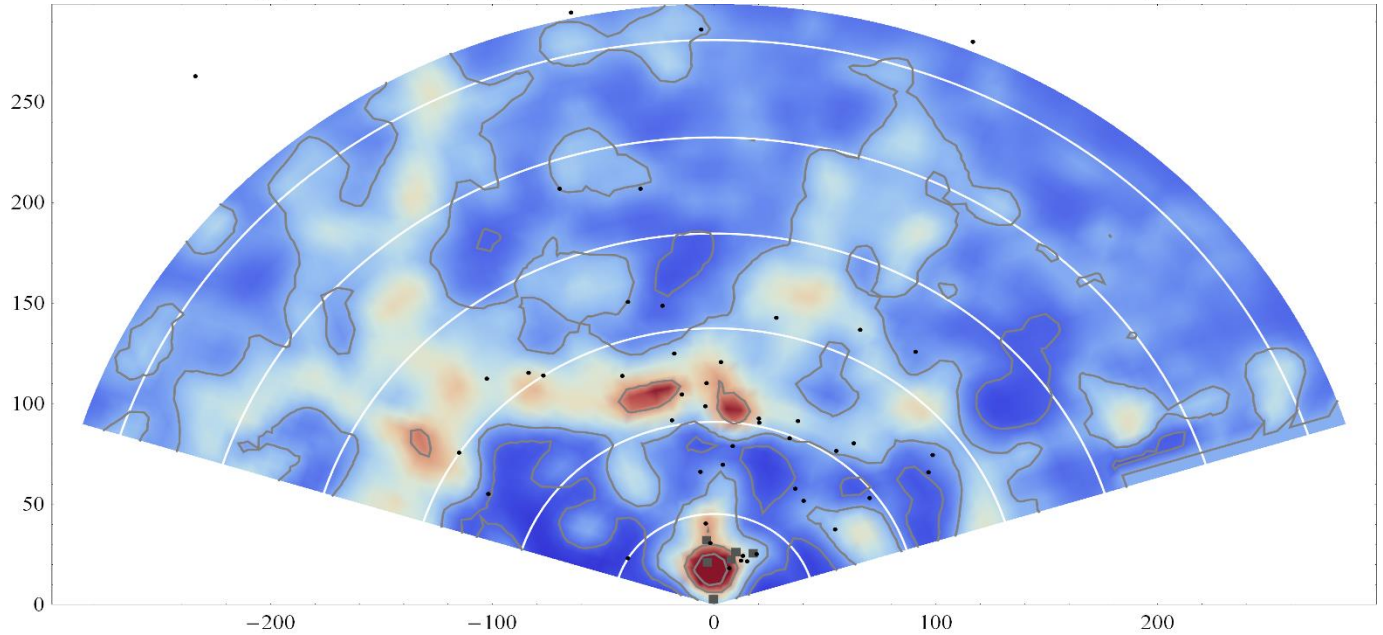

SN and Cepheids distribution in F1

Inversion method including non perturbative effects

$$\Delta = \frac{D_L^{\rm obs}}{D_L^{\rm Hom}} - 1 \equiv 10^{(\mu_{\rm obs} - \mu_{\rm Hom})/5} - 1$$

$$\delta_C^{\Lambda\rm LTB}(\Delta) = \frac{3}{f}\Delta + \frac{z}{f}\left(\frac{d\Delta}{dz} + 4\Delta\right),$$

$$\delta_C^{\rm LTB}(\Delta) = 3\Delta + z\left(\frac{d\Delta}{dz} + 4\Delta + 3\Omega_{\Lambda 0}\left(1 + \Delta\right)\right)$$

How good is the improved inversion for non linear structures?

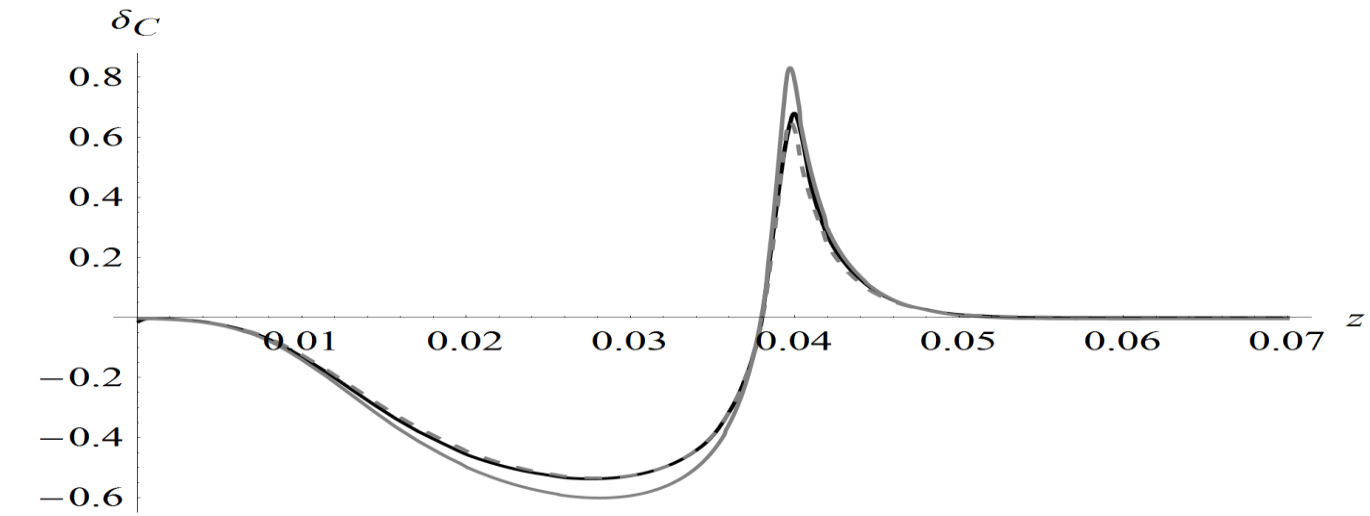

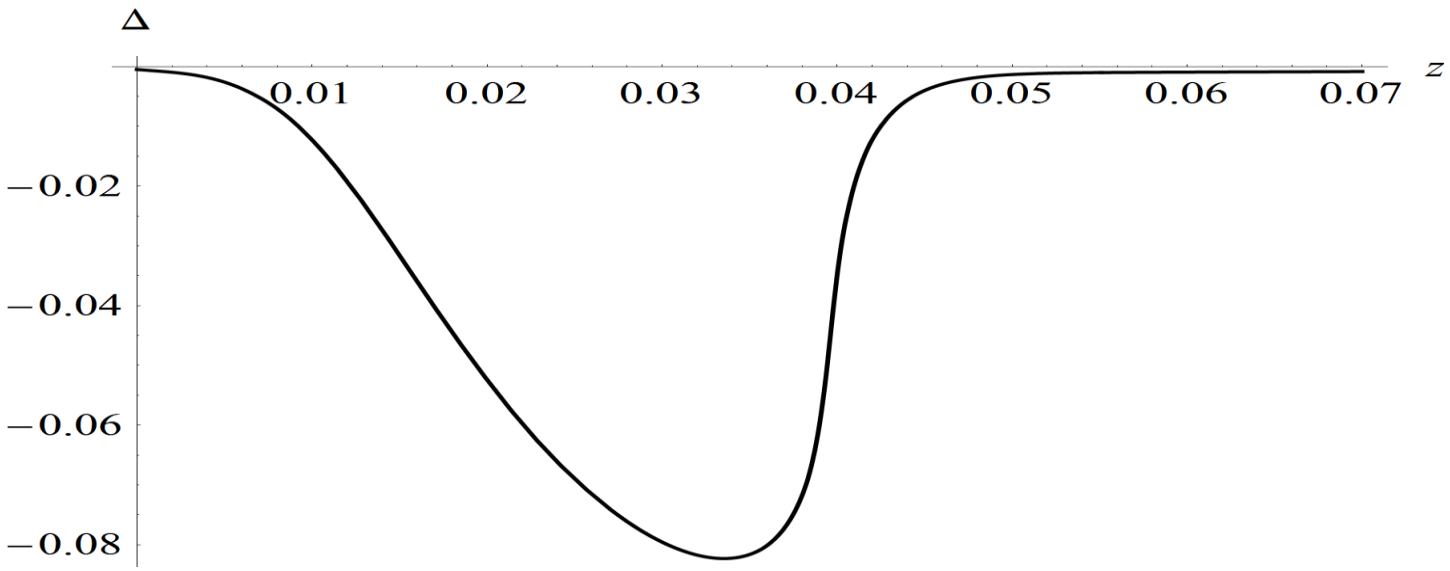

Improved inversion Solid line

Linear inversion Dashed line

Smoothing the input functions

- The inversion requires to differentiate the luminosity distance, and smooth functions are preferable
- In order to avoid any bias we make model independent fits of the distance modulus using radial basis functions (RBF) for the function f(z) defined

$$\left(\mu^{\mathrm{obs}} - \mu^{\mathrm{Planck}}\right)(z) \qquad\qquad (N_0, N_{-1}, N_{\mathrm{NL}})$$

$$f(z) = w_0 + w_{-1}\, z + \sum_{m=1}^{N_{\mathrm{NL}}} w_m\, \Phi\left(|z - p_m|\right) \qquad\qquad \Phi(r) = r^3.$$

- We fit w_0, w_1, the centers p_m, and the number of subintervals N_{NL} .
- A homogeneous model corresponds to al the parameters equal to zero.

Directional radial profiles reconstruction

- We divide SN in different sets, corresponding to Keenan's angular sub regions 1,2 3
- For each direction we reconstruct the density profile and compare it to Keenan and 2M++
- In the directions where there are enough data point we confirm Keenan's results and that 2M++ is not deep enough to detect these inhomogeneities
- If SN were red-shift corrected with our reconstructed density/velocity profiles the discrepancy would be removed, as anticipated by previous theoretical predictions
- There is no tension! There is just a local structure that galaxy catalogs have not detected due to their limited depth
- Euclid could provide very important confirmations both in terms of new and more accurate SN luminosity distance observations and number counts

Results for subregions 1 and 3

For F1, the best fitting model we get without removing any outlier and with $z_{\max} = 0.2$, is

$$(1, 0, 0) \text{ model with } H_0^{\rm loc} = 72.90 \pm 0.51 \text{ km s}^{-1} \text{ Mpc}^{-1}$$

- Subregion 3

$z_{\max} = 0.2$					$z_{\max} = 0.4$				
Fig.	χ^2_R	*Threshold* (%)	*Param.*	Removal	Fig.	χ^2_R	*Threshold* (%)	*Param.*	Removal
9	1.40	39 ~ 100	(0, 0, 5)		9	1.43	38 ~ 100	(0, 1, 5)	
N/A	3.45	97.5 ~ 100	(0, 0, 0)	NGC 4536	N/A	3.31	92.6 ~ 100	(0, 0, 0)	NGC 4536
10(a)	2.26	89 ~ 97.4	(1, 0, 1)	Same	11(a)	2.20	92.1 ~ 92.5	(0, 1, 2)	Same
N/A	2.88	99.5 ~ 100	(0, 0, 0)	+1999cl	N/A	2.80	96.3 ~ 100	(0, 0, 0)	+1999cl
10(b)	1.55	94.1 ~ 99.4	(1, 0, 1)	Same	11(b)	1.96	89 ~ 96.2	(1, 0, 1)	Same
10(c)	**1.47**	**47 ~ 94.0**	**(0, 0, 2)**	**Same**	11(c)	**1.37**	**76 ~ 88**	**(0, 0, 4)**	**Same**

Field 3 reconstruction, zmax=0.4

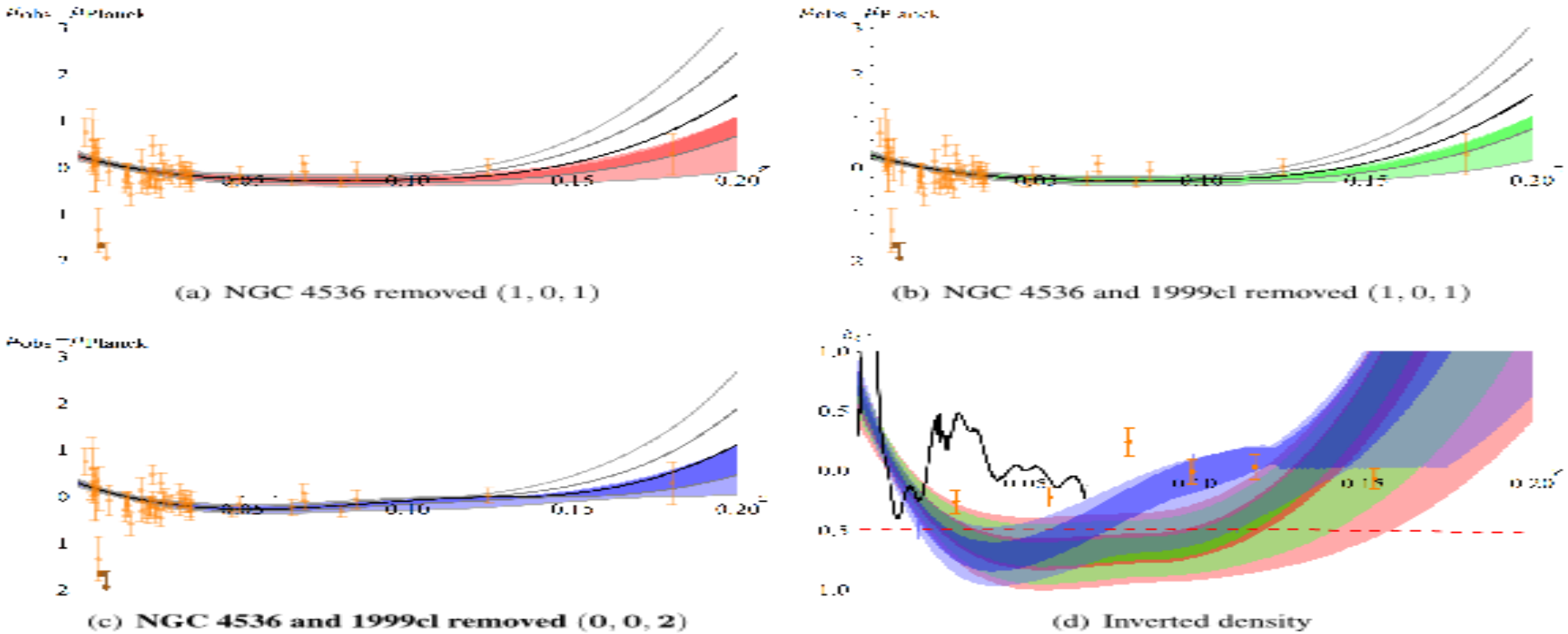

(a) NGC 4536 removed (1, 0, 1)

(b) NGC 4536 and 1999cl removed (1, 0, 1)

(c) **NGC 4536 and 1999cl removed (0, 0, 2)**

(d) Inverted density

Figure 10. Distance modulus best fit models are plotted for F3 with $z_{\max} = 0.2$, without peculiar velocity corrections and with a 250 km s^{-1} velocity dispersion for SNe. The model parameters and the removed data points are shown in the sub-captions. (a, b, c): Standard candles distance modulus data are plotted with their best fit (black), 68% (gray) and 95% (light gray) confidence bands according to the method of section 3. The invertible bands are shown as the shaded region (68%-darker color, 95%-lighter color), while the removed outliers are shown as darker data points. Case (c) is preferred. (d): The confidence bands of the inverted density contrast corresponding to the invertible bands of the distance modulus are shown (68%-darker color, 95%-lighter color). The data points of $\mathcal{K}13$ are plotted in orange, the 2M++ density contrast averaged over F3 as a solid black curve, and the dashed red line is for density contrast that would lead to a local Hubble parameter $H_0^{\rm loc} = H_0^{\rm Riess}$ assuming a large scale $H_0^{LS} = H_0^{\rm Planck}$. The bands are color coded case by case with red (a), green (b), blue (c).

Field 3 reconstruction, zmax=0.4

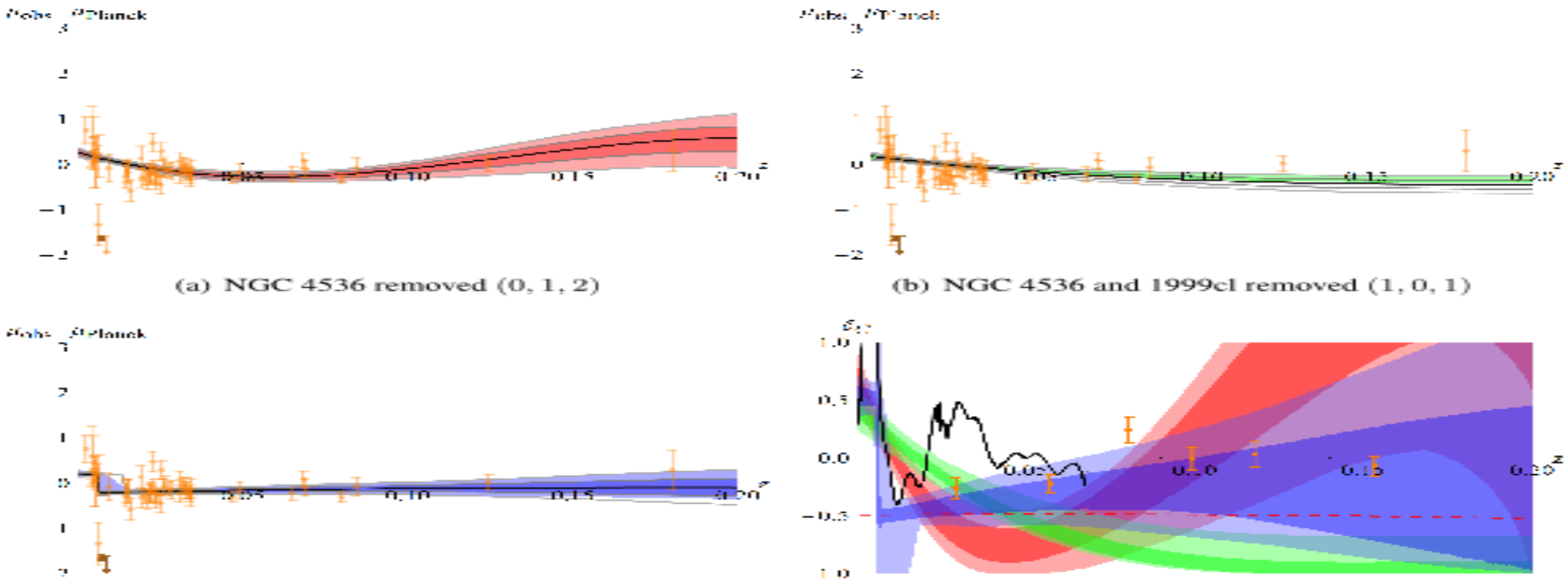

(a) NGC 4536 removed (0, 1, 2)

(b) NGC 4536 and 1999cl removed (1, 0, 1)

(c) **NGC 4536 and 1999cl removed** (0, 0, 4)

(d) Inverted density

Figure 11. Distance modulus best fit models are plotted for F3 with $z_{\max} = 0.4$, without peculiar velocity corrections and with a 250 $\mathrm{km\,s^{-1}}$ velocity dispersion for SNe. The model parameters and the removed data points are shown in the sub-captions. (a, b, c): Standard candles distance modulus data are plotted with their best fit (black), 68% (gray) and 95% (light gray) confidence bands according to the method of section 3. The invertible bands are shown as the shaded region (68%-darker color, 95%-lighter color), while the removed outliers are shown as darker data points. Case (c) is preferred. (d): The confidence bands of the inverted density contrast corresponding to the invertible bands of the distance modulus are shown (68%-darker color, 95%-lighter color). The data points of $\mathcal{K}13$ are plotted in orange, the 2M++ density contrast averaged over F3 as a solid black curve, and the dashed red line is for density contrast that would lead to a local Hubble parameter $H_0^{\rm loc} = H_0^{\rm Riess}$ assuming a large scale $H_0^{LS} = H_0^{\rm Planck}$. The bands are color coded case by case with red (a), green (b), blue (c).

Field 1 reconstruction, zmax=0.2

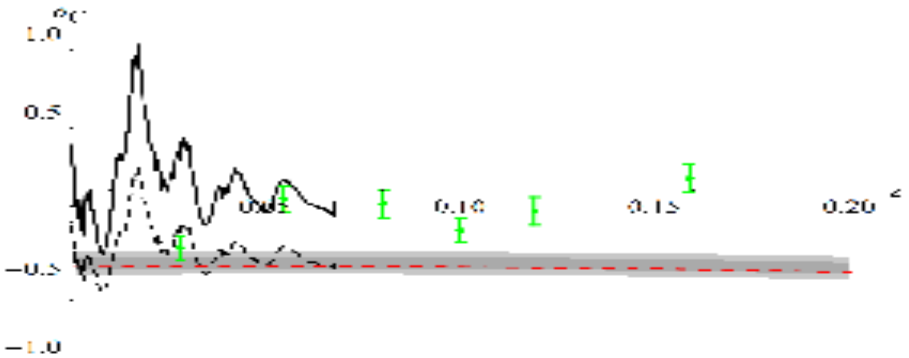

(a) Subregion F1 (1, 0, 0)

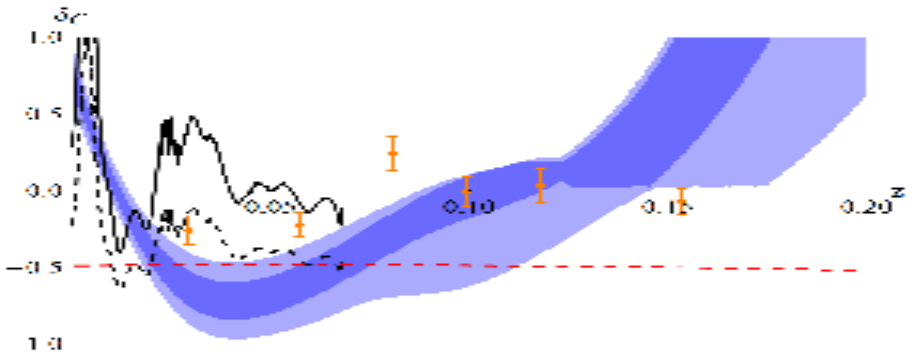

(b) Subregion F3 $z_{\max} = 0.2$ with NGC 4536 and 1999cl removed (0, 0, 2)

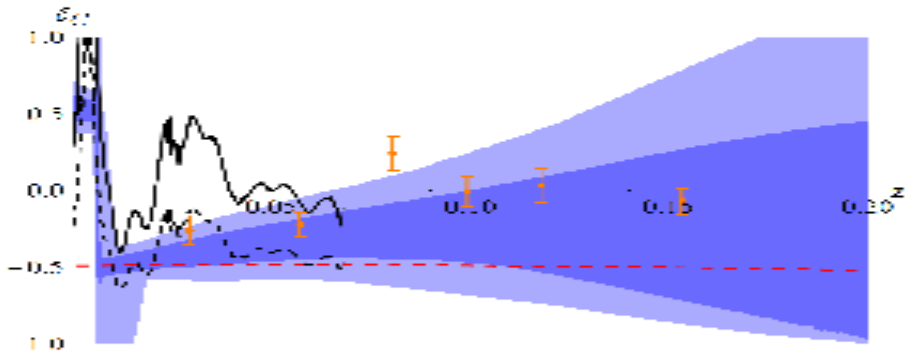

(c) Subregion F3 $z_{\max} = 0.4$ with NGC 4536 and 1999cl removed (0, 0, 4)

Figure 12. The confidence bands of the inverted density contrast for the standard candles distance modulus data without peculiar velocity corrections and with a 250 km s^{-1} velocity dispersion for SNe are shown (68%-darker color, 95%-lighter color). The model parameters and the cuts of the dataset are shown in the sub-captions. In addition the data points of $\mathcal{K}13$ are plotted in orange for F3 and green for F1, the 2M++ density contrast averaged over the subregion specified in the sub-captions as a solid black curve, its rescaled version by a factor of 0.6 according to $\mathcal{K}13$ as a dashed black curve, and the dashed red line is for density contrast that would lead to a local Hubble parameter $H_0^{\rm loc} = H_0^{\rm Riess}$ assuming a large scale $H_0^{LS} = H_0^{\rm Planck}$.

Field 1 reconstruction, zmax=0.4

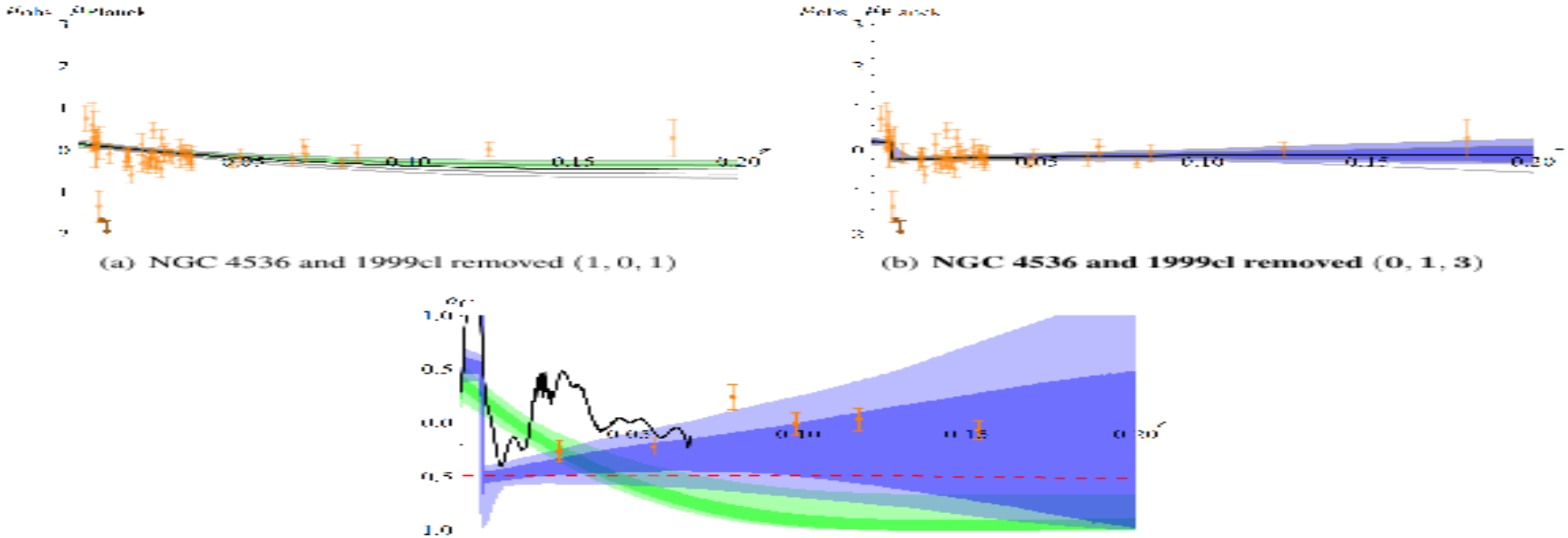

(a) NGC 4536 and 1999cl removed (1, 0, 1)

(b) **NGC 4536 and 1999cl removed (0, 1, 3)**

(c) Inverted density

Figure 15. Distance modulus best fit models are plotted for F3 with $z_{\max} = 0.4$, without peculiar velocity corrections and without velocity dispersion. The model parameters and the removed data points are shown in the sub-captions. (a, b): Standard candles distance modulus data are plotted with their best fit (black), 68% (gray) and 95% (light gray) confidence bands according to the method of section 3. The invertible bands are shown as the shaded region (68%-darker color, 95%-lighter color), while the removed outliers are shown as darker data points. Case (b) is preferred. (c): The confidence bands of the inverted density contrast corresponding to the invertible bands of the distance modulus are shown (68%-darker color, 95%-lighter color). The data points of $\mathcal{K}13$ are plotted in orange, the 2M++ density contrast averaged over F3 as a solid black curve, and the dashed red line is for density contrast that would lead to a local Hubble parameter $H_0^{\rm loc} = H_0^{\rm Riess}$ assuming a large scale $H_0^{LS} = H_0^{\rm Planck}$. The bands are color coded case by case with green (a) and blue (b).

Conclusions

- The reconstruction is in agreement with Kenan at low redshift
- Further evidence of anisotropy
- More data will make it possible to reconstruct the density in other directions such as F3
- A more general reconstruction method can be developed
- SN provide a unique window on high red-shift large scale structure, in particular on dark matter, because gravitational effects are the same for DM and baryonic matter, but at high red-shift selection effects make baryonic matter observations more difficult
- The reconstruction gives the correct normalization with respect to the average density of the Universe for galaxy surveys such as 2M++, which are limited by their depth